# Influenza A Virus Inhibits Alveolar Fluid Clearance in BALB/c Mice

**Kendra E. Wolk[1], Eduardo R. Lazarowski[2], Zachary P. Traylor[1], Erin N. Z. Yu[1], Nancy A. Jewell[3,4], Russell K. Durbin[3], Joan E. Durbin[3,4], and Ian C. Davis[1]**

[1]Department of Veterinary Biosciences, Ohio State University, Columbus, Ohio; [2]Department of Medicine, University of North Carolina, Chapel Hill, North Carolina; [3]Columbus Children's Research Institute, Columbus, Ohio; and [4]Department of Pediatrics, Ohio State University, Columbus, Ohio

***Rationale*: Pulmonary infections can impair alveolar fluid clearance (AFC), contributing to formation of lung edema. Effects of influenza A virus (IAV) on AFC are unknown.**

***Objectives*: To determine effects of IAV infection on AFC, and to identify intercellular signaling mechanisms underlying influenza-mediated inhibition of AFC.**

***Methods*: BALB/c mice were infected intranasally with influenza A/WSN/33 (10,000 or 2,500 focus-forming units per mouse). AFC was measured in anesthetized, ventilated mice by instilling 5% bovine serum albumin into the dependent lung.**

***Measurements and Main Results*: Infection with high-dose IAV resulted in a steady decline in arterial oxygen saturation and increased lung water content. AFC was significantly inhibited starting 1 hour after infection, and remained suppressed through Day 6. AFC inhibition at early time points (1–4 h after infection) did not require viral replication, whereas AFC inhibition later in infection was replication-dependent. Low-dose IAV infection impaired AFC for 10 days, but induced only mild hypoxemia. High-dose IAV infection increased bronchoalveolar lavage fluid ATP and UTP levels. Impaired AFC at Day 2 resulted primarily from reduced amiloride-sensitive AFC, mediated by increased activation of the pyrimidine-P2Y purinergic receptor axis. However, an additional component of AFC impairment was due to activation of $A_1$ adenosine receptors and stimulation of increased cystic fibrosis transmembrane regulator–mediated anion secretion. Finally, IAV-mediated inhibition of AFC at Day 2 could be reversed by addition of β-adrenergic agonists to the AFC instillate.**

***Conclusions*: AFC inhibition may be an important feature of early IAV infection. Its blockade may reduce the severity of pulmonary edema and hypoxemia associated with influenza pneumonia.**

**Keywords:** orthomyxovirus infections; pneumonia, viral; pulmonary edema; ion transport; adenosine

## AT A GLANCE COMMENTARY

### Scientific Knowledge on the Subject

Active transport of sodium ions by bronchoalveolar epithelial cells drives alveolar fluid clearance (AFC), which is crucial to efficient gas exchange in the lung.

### What This Study Adds to the Field

Infection with influenza A virus has physiologically significant inhibitory effects on AFC *in vivo* in BALB/c mice, which result from uridine diphosphate–mediated inhibition of sodium transport and adenosine-mediated stimulation of chloride secretion.

Influenza A virus (IAV) causes a highly contagious, acute respiratory disease in humans (1). Most IAV infections are self-limiting, but pneumonia and cardiac complications can lead to significant morbidity and mortality (1). Furthermore, novel, highly virulent IAV strains can arise after genetic reassortment between strains (antigenic shift) (1). The resultant IAV pandemics elicited devastating loss of life throughout the 20th century, and have the potential to do so in the 21st (2). Antiviral drugs are available for IAV, but may be of limited long-term utility due to development of viral resistance mutants (1). Vaccination remains central to IAV control, but continued antigenic drift necessitates the development of new vaccines each year. Moreover, its utility in the elderly has recently been questioned (3).

To facilitate normal gas exchange and effective mucociliary clearance in the lung, the depth of the thin layer of fluid that lines the airspaces is tightly regulated, and is a direct reflection of the ion transport function of the respiratory epithelium. Normally, the dominant ion transport process of the bronchoalveolar epithelium is active transport of sodium ($Na^+$) ions from the alveolar lining fluid (ALF) to the subepithelial interstitial space (4). $Na^+$ ions in the ALF enter epithelial cells by passive diffusion through apical membrane epithelial $Na^+$ channels (ENaC). The favorable electrochemical gradient for $Na^+$ influx is maintained by the basolateral $Na^+/K^+$ ATPase, which uses the energy from ATP hydrolysis to transport three intracellular $Na^+$ ions into the interstitial space in exchange for two extracellular potassium ($K^+$) ions. Chloride ($Cl^-$) ions follow transepithelial $Na^+$ movement (via paracellular pathways and apical membrane cystic fibrosis transmembrane regulator [CFTR] $Cl^-$ channels) to maintain electrical neutrality. Transport of NaCl creates a transepithelial osmotic gradient, which causes water to move passively from the ALF to the interstitium. Inhibition of the $Na^+$ transport process can result in formation of an excessive volume of ALF and impairment of gas exchange (5).

Exposure of murine tracheal tissue to pneumotropic IAV or free viral hemagglutinins has been shown to result in rapid inhibition of active $Na^+$ transport (within 60 min) (6). IAV has also been shown to reduce ENaC activity in rat alveolar type II cells over a comparable time period (7). However, it is not clear how these effects correlate to those of IAV replication within the lung over a period of several days, as would occur in an infected subject. We therefore used a BALB/c mouse model to investigate the effects of IAV infection on alveolar fluid clearance (AFC), which is an *in vivo* measure of active transepithelial ion transport. Some of the results of

(*Received in original form March 24, 2008; accepted in final form July 22, 2008*)

Supported by National Institutes of Health grant RR17626 (I.C.D.) and funds from Ohio State University.

Correspondence and requests for reprints should be addressed to Ian C. Davis, D.V.M., Ph.D., Department of Veterinary Biosciences, Ohio State University, 331 Goss Lab, 1925 Coffey Road, Columbus, OH 43210. E-mail: davis.2448@osu.edu

This article has an online supplement, which is available from the issue's table of contents at www.atsjournals.org

**Am J Respir Crit Care Med Vol 178. pp 969–976, 2008**
**Originally Published in Press as DOI: 10.1164/rccm.200803-455OC on August 8, 2008**
**Internet address: www.atsjournals.org**

these studies have been previously reported in the form of an abstract (8).

## METHODS

### Reagents

Except where noted, all reagents were from Sigma-Aldrich (St. Louis, MO). Amiloride, A77–1726 (EMD Biosciences, La Jolla, CA), genistein, fluoxetine, glibenclamide, forskolin, $CFTR_{inh}$-172 (EMD Biosciences), and 8-cyclopentyl-1,3-dipropylxanthine (Tocris Bioscience, Ellisville, MO) were reconstituted in dimethyl sulfoxide. Niflumic acid was reconstituted in acetone. 4,4′-Diisothiocyanostilbene-2,2′-disulfonic acid (DIDS) was reconstituted in 0.1 M potassium bicarbonate, pH 8.0. Rho kinase (ROCK) inhibitor and XAMR-0721 (both EMD Biosciences), *N*-(4-cyanophenyl)-2-[4-(2,3,6,7-tetrahydro-2,6-dioxo-1,3-dipropyl-1H-purin-8-yl) phenoxy]-acetamide (MRS 1754; Tocris Bioscience), and all other reagents used were reconstituted in normal saline. Reagents were added to the AFC instillate from stock solution aliquots immediately before instillation into mice, in a minimal volume of solvent (1–10 μl/ml).

### Preparation of Viral Inocula

Influenza A/WSN/33 (H1N1) virus (WSN [Wisconsin] virus; a mouse-adapted H1N1 human IAV strain, which is pneumotropic after intranasal inoculation [9]) was grown in Madin-Darby bovine kidney cells, and its infectivity assayed by fluorescent-focus assay 24 hours after inoculation of the NY3 fibroblast cell line (derived from signal transducer and activator of transcription-$1^{-/-}$ mice), as previously described (10). Aliquots of WSN stocks, diluted identically to live stocks, were inactivated by exposure to 1,800 mJ of radiation in a Stratalinker UV crosslinker (Stratagene, La Jolla, CA) (10).

### Infection of Mice

Pathogen-free, 8- to 12-week-old BALB/c mice of either sex (maintained in sterile caging) were infected intranasally with 50 μl influenza A/WSN/33 under light ketamine/xylazine anesthesia, as previously described (11). Mock-infected animals received 50 μl of virus diluent (phosphate-buffered saline with 0.1% bovine serum albumin [BSA]). In some experiments, mice were individually marked and weighed daily. All mouse procedures were approved by the Institutional Animal Care and Use Committee at Ohio State University.

### AFC Measurements

AFC was measured as previously described (11), but with correction for excess murine alveolar protein, as described in the supplemental methods. In all studies, four ventilators were run concurrently (with the procedure staggered by a 3-min interval). Data for each experimental group were derived from a minimum of two independent infections. We found no sex-associated difference in AFC rate in BALB/c mice.

### Measurement of Bronchoalveolar Epithelial Permeability

AFC procedures were performed using a 5% BSA solution containing 0.16 mg/ml fluorescein isothiocyanate (FITC)–tagged albumin (Sigma-Aldrich). The amount of FITC-albumin detectable in peripheral serum at the end of the AFC procedure was measured at 520 nm (excitation, 487 nm) in a NanoDrop 1000 fluorescence spectrometer (Thermo Scientific, Wilmington, DE) (12).

### Measurement of Bronchoalveolar Lavage Proinflammatory Mediators

Cytokines and chemokines were measured by ultrasensitive mouse proinflammatory multiplex electrochemiluminescence assay (Meso Scale Discovery, Gaithersburg, MD). Total nitrate/nitrite was measured by fluorometric assay (Cayman Chemical, Ann Arbor, MI). Lactate dehydrogenase was measured by colorimetric assay (Cayman Chemical). All assays were performed in accordance with manufacturer's instructions.

### Other Methods

All other methods were performed as previously described (10, 11).

### Statistical Analyses

Descriptive statistics were calculated using Instat 3.05 (GraphPad Software, San Diego, CA). Gaussian data distribution was verified by the method of Kolmogorov and Smirnov. Differences between group means were analyzed by analysis of variance, with Tukey-Kramer multiple comparison post-tests. Correlations were calculated by Pearson's linear correlation analysis. $P < 0.05$ was considered statistically significant. All data are presented as mean ± SEM.

## RESULTS

### Effects of IAV on Body Weight in BALB/c Mice

Mock infection had no effect on body weight in BALB/c mice (Figure 1A). Intranasal infection with 10,000 focus-forming units (FFU) per mouse of WSN virus (influenza A/WSN/33) caused a significant decline in body weight beginning 2 days after infection, together with ruffling of fur, hunched posture, and reduced activity. By Day 5, mice had lost over 20% of starting weight and appeared moribund. A further precipitous decline in weight occurred between Days 5 and 6, necessitating termination of studies by Day 6. These findings were comparable to those previously reported for mice infected with this IAV strain at this titer (13). Infection of mice with an equivalent dose of ultraviolet (UV)-inactivated WSN virus had no effect on body weight, whereas infection with a sublethal dose (2,500 FFU/mouse) of live virus only induced significant weight loss at Days 1 and 2 after infection.

Despite inducing severe cachexia, infection with 10,000 FFU/mouse WSN virus did not alter either serum albumin or osmolality—a small increase in serum osmolality was detected at Day 1, but this was probably related to water deprivation associated with recovery from general anesthesia at Day 0, as it was also observed in mock-infected mice at this time point (14) (Figures E1A and E1B in the online supplement).

### Effect of IAV on Peripheral Blood Oxygen Saturation

Mock infection had no effect on peripheral blood oxygen saturation ($Sp_{O_2}$) in conscious BALB/c mice. However, infection with 10,000 FFU/mouse WSN virus resulted in mild hypoxemia from Day 2 postinfection (Figure 1B). Hypoxemia became particularly severe at Day 6, when mice were moribund. This rapid progression of hypoxemia was similar to that reported by Sidwell and colleagues in WSN virus–infected mice (15). Infection with an equivalent dose of UV-inactivated WSN virus had no effect on $Sp_{O_2}$, whereas infection with 2,500 FFU/mouse of live virus only induced significant hypoxemia at Days 1 and 2 after infection.

### IAV Replication in Lungs of BALB/c Mice

IAV replication was detectable in lung homogenates at 1 day after infection with 10,000 FFU virus and peaked at Day 2 (Figure 1C). Replication was significantly lower at Day 4, and was comparable to Day 1 by 6 days after infection. Infection with 2,500 FFU/mouse WSN virus resulted in similar replication kinetics in mouse lungs, with significant viral titers detectable out to Day 10. In mice infected with an equivalent dose of UV-inactivated virus, titers at Day 2 were reduced by more than 4 logs—very limited residual replication (<140 FFU/g lung weight) was detectable.

### Effects of IAV on Lung Water Content

Infection with 10,000 FFU/mouse WSN virus for 1–6 days, or with 2,500 FFU/mouse WSN virus for 1 to 8 days, resulted in a significant increase in lung wet:dry weight ratios compared with mock-infected mice (Figure 1D). There was a significant

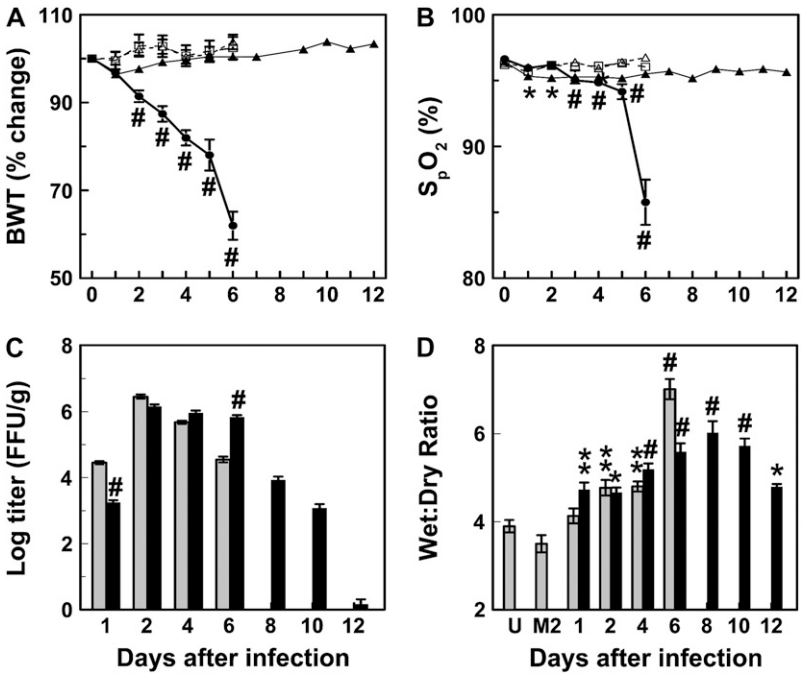


***Figure 1.*** Influenza A WSN virus infection of BALB/c mice. (*A*) Percentage change in body weight (BWT) after mock infection (*open triangles*), infection with 10,000 focus-forming units (FFU) per mouse WSN virus (WSN 10) (*solid circles*), infection with 2,500 FFU/mouse WSN virus (WSN 2.5) (*solid triangles*), or infection with 10,000 FFU/mouse ultraviolet (UV)-inactivated WSN (UV-WSN) (*open squares*) virus (n = 10 for mock-infected mice; n = 15–60 for WSN-infected mice; n = 10 for UV-WSN–infected mice). $^{\#}P < 0.0005$ compared with Day 0 BWT. (*B*) Effect of mock infection (*open triangles*), infection with WSN 10 (*solid circles*), infection with WSN 2.5 (*solid triangles*), or infection with 10,000 FFU/mouse UV-WSN (*open squares*) on peripheral arterial $O_2$ saturation ($Sp_{O_2}$) (n = 9–20 for mock-infected mice; n = 12–25 for WSN-infected mice; n = 10–30 for UV-WSN–infected mice). $^{*}P < 0.05$, $^{\#}P < 0.0005$, compared with Day 0 $Sp_{O_2}$ for the same group. (*C*) Replication of WSN virus in lung homogenates after infection with WSN 10 (*shaded bars*) or WSN 2.5 (*solid bars*) (n = 5–13 per time point). $^{\#}P < 0.0005$ compared with 10,000 FFU/mouse titer at the same time point. (*D*) Effect of mock infection for 2 days (M2), infection with WSN 10 (*shaded bars*), or infection with WSN 2.5 (*solid bars*) on lung water content, as measured by wet:dry ratio (n = 5–8 per group). $^{*}P < 0.05$, $^{**}P < 0.005$, $^{\#}P < 0.0005$, compared with uninfected mice (U).

correlation ($P < 0.005$; $r^2 = 0.546$; n = 13) between mean lung water content and mean $Sp_{O_2}$ after WSN virus infection.

### Effects of IAV on Bronchoalveolar Epithelial Integrity

Bronchoalveolar lavage (BAL) lactate dehydrogenase and protein content were not elevated above levels in mock-infected mice until Day 6 after infection with 10,000 FFU/mouse WSN virus (Figures E2A and E2B). Measurements of the flux of FITC-conjugated BSA from the instillate to the bloodstream over a 30-minute period confirmed that WSN virus does not induce significant increases in alveolar permeability until 4 to 6 days after infection (Figure E2C). At these time points, small amounts of murine albumin could also be detected in AFC aspirates (Figure E2D).

An independent observer found no histopathologic evidence of any epithelial cell death or sloughing of epithelium until Day 4 after WSN virus infection. Likewise, terminal deoxynucleotidyl transferase–mediated dUTP nick end-labeling analysis indicated that epithelial apoptosis was restricted to sporadic small foci at Day 2 and was not widespread until Day 4 (Figures E2E and E2F). IAV antigen was detected predominantly in bronchiolar epithelium at Day 2, but widespread immunoreactivity in alveolar epithelial cells and alveolar macrophages was seen at Day 4 (Figures E2G and E2H).

### Effect of IAV on BAL Proinflammatory Mediator Levels in BALB/c Mice

Infection with 10,000 FFU/mouse WSN virus increased BAL proinflammatory cytokine levels with comparable kinetics to those of previous reports (16–18) (Figure E3). No change in BAL nitrate/nitrite levels was detected at any time point (data not shown).

### Effects of IAV on AFC in BALB/c Mice

AFC was evaluated in live mice with normal oxygenation and acid–base balance, as previously described (11). The basal AFC rate in mice that were mock infected for 2 days was not different from that in uninfected mice (Figure 2A), and was identical to that which we have reported previously for BALB/c mice (11, 19, 20). AFC was significantly depressed (by 27% from the mean rate in mock-infected mice) by Day 1 after infection with 10,000 FFU/mouse of WSN virus, and further decreased at Day 2 (by 52% from the mean rate in mock-infected mice). No recovery of basal AFC rate was detected at Days 4 and 6 postinfection. The ENaC inhibitor amiloride (1.5 mM) reduced the mean AFC rate to 12% in both mock-infected and WSN virus–infected mice at Day 2 (Figure 2B). When mice were challenged with an equivalent dose of UV-inactivated virus, AFC was reduced at 2 and 4 days after infection, but not at Days 1 or 6 (Figure 2C). However, the inhibitory effect of UV-inactivated WSN virus on AFC at Days 2 and 4 was small and significantly less than that induced by 10,000 FFU/mouse live virus at the same time points (both $P < 0.005$).

Infection with 2,500 FFU/mouse of live WSN virus resulted in a similar rapid decline in basal AFC rate (by 46% at Day 1 and 62% at Day 2) to that seen in mice infected with 10,000 FFU virus (Figure 2C). AFC remained significantly depressed in these mice until Day 8 after infection, and did not fully recover until Day 18. Finally, there was a significant correlation between mean AFC rate and mean $Sp_{O_2}$ ($P < 0.001$; $r^2 = 0.652$; n = 13) after WSN virus infection.

Because Kunzelmann and colleagues (6) had described very rapid inhibitory effects of pneumotropic IAV on active $Na^+$ transport by mouse tracheal tissue, we also examined the effects of short-term challenge with WSN virus (10,000 FFU/mouse) on AFC. Whereas mock infection had a small (but nonsignificant) inhibitory effect upon AFC at 1 to 4 hours after infection, WSN virus caused much greater AFC inhibition (Figure 2D). AFC was reduced by 47% from the mean rate in mock-infected mice at 1 hour after infection, and remained significantly impaired at 4 hours. Challenge with an equivalent dose of UV-inactivated virus resulted in a comparable reduction in AFC at 1 to 4 hours after infection. WSN virus–induced AFC inhibition at 1 hour after infection could be completely reversed by the protein kinase C inhibitor, bisindolylmaleimide 1 hydrochloride (BIM-1) (100 μM).

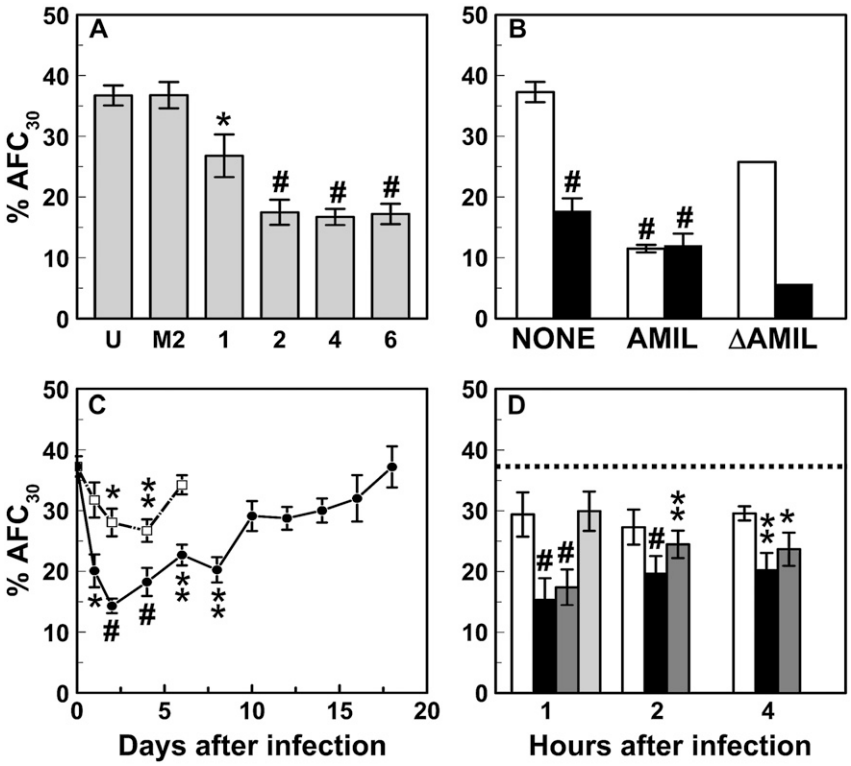


*Figure 2.* Effect of influenza A virus (IAV) infection on alveolar fluid clearance (AFC). (*A*) Effect of mock infection or infection with 10,000 FFU/mouse WSN virus for 1–6 days on basal AFC (n = 12 for uninfected mice [U]; n = 8 for mock-infected mice at Day 2 [M2]; n = 10 for WSN-infected mice at Day 1; n = 11 for WSN-infected mice at Day 2; n = 9 for WSN-infected mice at Day 4; n = 17 for WSN-infected mice at Day 6). $^{*}P < 0.05$, $^{\#}P < 0.0005$, compared with mock-infected mice. (*B*) Effect of mock infection (*open bars*) or infection with WSN 10 (*solid bars*) on AFC sensitivity to amiloride (AMIL; 1.5 mM) at Day 2 (n = 7–8 per group, except n = 11 for untreated, WSN-infected mice). ΔAMIL = % mean basal AFC − % mean amiloride-insensitive AFC. $^{\#}P < 0.0005$ compared with untreated, mock-infected mice. (*C*) Effect of infection with 2,500 FFU/mouse live WSN virus (*solid circles*) or 10,000 FFU/mouse UV-inactivated WSN virus (*open squares*) on basal AFC (n = 7–9 per time point). $^{*}P < 0.05$, $^{**}P < 0.005$, $^{\#}P < 0.0005$, compared with mock-infected mice. (*D*) Effect of mock infection (*open bars*), infection with 10,000 FFU/mouse WSN virus (*solid bars*), or infection with an equivalent dose of UV-inactivated WSN virus (*dark shaded bars*) for 1–4 hours on AFC (n = 7–9 per group). Also shown is the effect of the protein kinase C inhibitor, bisindolylmaleimide 1 hydrochloride (BIM-1) (100 μM) (*light shaded bars*), on AFC at 1 hour after infection with WSN 10 (n = 10). *Dotted line* indicates mean AFC rate in uninfected animals (n = 8). $^{*}P < 0.05$, $^{**}P < 0.005$, $^{\#}P < 0.0005$, compared with uninfected animals.

### Effect of IAV on BAL 5′-Nucleotide Levels

Infection of BALB/c mice with the paramyxovirus respiratory syncytial virus (RSV) results in increased release of *de novo*–synthesized UTP into the bronchoalveolar space, which mediates AFC inhibition (11, 20). BAL fluid from uninfected or mock-infected mice contained equivalent levels of ATP and UTP. Infection with 10,000 FFU/mouse of WSN virus resulted in a significant increase in BAL levels of both ATP and UTP at Days 1 and 2, but not Day 4 (Figure 3). BAL ATP and UTP levels decreased again at Day 4 after infection.

### Effect of Blockade of the Pyrimidine–Purinergic Receptor Axis on IAV-mediated Inhibition of AFC at Day 2 after Infection

In order to determine the role of 5′-nucleotide–mediated P2Y purinergic receptor activation in mediating the inhibitory effects of WSN virus on AFC, we evaluated mice infected with 10,000 FFU/mouse WSN virus at the Day 2 time point, when inhibition of AFC was maximal, but epithelial damage was not yet severe. We had previously demonstrated that none of the agents used in this part of the study have any effect on basal AFC rate in normal mice (11, 20).

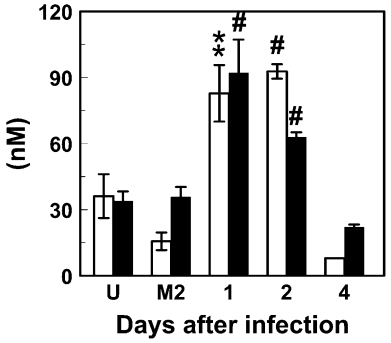


*Figure 3.* Effect of mock infection for 2 days (M2) or infection with influenza A virus (IAV) for 1–4 days on bronchoalveolar lavage ATP (*open bars*) and UTP (*solid bars*) levels (n = 7–8 per group). Values are corrected for lung water. $^{**}P < 0.005$, $^{\#}P < 0.0005$, compared with uninfected animals (U).

The *de novo* pyrimidine synthesis inhibitor, A77–1726 (20 μM), reversed WSN virus–induced suppression of AFC at Day 2 (Figure 4A) by stimulating amiloride-sensitive transport. Dihydro-orotate dehydrogenase inhibitors, such as A77–1726, also have nonspecific tyrosine kinase inhibitory activity (21). However, the beneficial effect of A77–1726 on AFC at Day 2 was not replicated by the broad-spectrum tyrosine kinase inhibitor, genistein (20 μM). Furthermore, blockade of IAV-mediated AFC inhibition by A77–1726 was partially reversed by 20 μM uridine, which allows pyrimidine synthesis via a salvage pathway, indicating that the A77–1726 block is specific to the *de novo* pyrimidine synthesis pathway.

Volume-regulated anion channels (VRACs) have been shown to mediate ATP release from respiratory epithelial cells *in vitro* (22). WSN virus–mediated inhibition of AFC at Day 2 was partially blocked by the proposed VRAC inhibitor, fluoxetine (10 μM) (23), and this block was reversed by 500 nM UTP (Figure 4B). VRAC opening can be facilitated by Rho kinase activation (24). The Rho kinase inhibitor (ROCKi) (50 μM) also partially blocked inhibition of basal AFC at Day 2 after WSN virus infection.

Functional evidence suggests that murine lung epithelial cells express $P2Y_2$ and $P2Y_6$ purinergic receptors (25): activation of these receptors by 5′-nucleotides (ATP/UTP and UDP, respectively) results in impaired epithelial $Na^+$ transport (26). AFC at Day 2 after WSN virus infection was significantly increased by apyrase (5 U/ml), which degrades ATP and UTP to their monophosphate forms, but was unaffected by hexokinase (5 U/ml with 10 mM glucose), which hydrolyzes ATP and UTP to their diphosphate forms (27) (Figure 4C). UDP-glucose-pyrophosphorylase (5 U/ml with 5 U/ml inorganic pyrophosphatase and 10 mM glucose-1-phosphate), which metabolizes UTP to UDP-glucose, also significantly increased AFC at Day 2 (Figure 4C). This effect was lost in the absence of inorganic pyrophosphatase, which provides the energy to drive

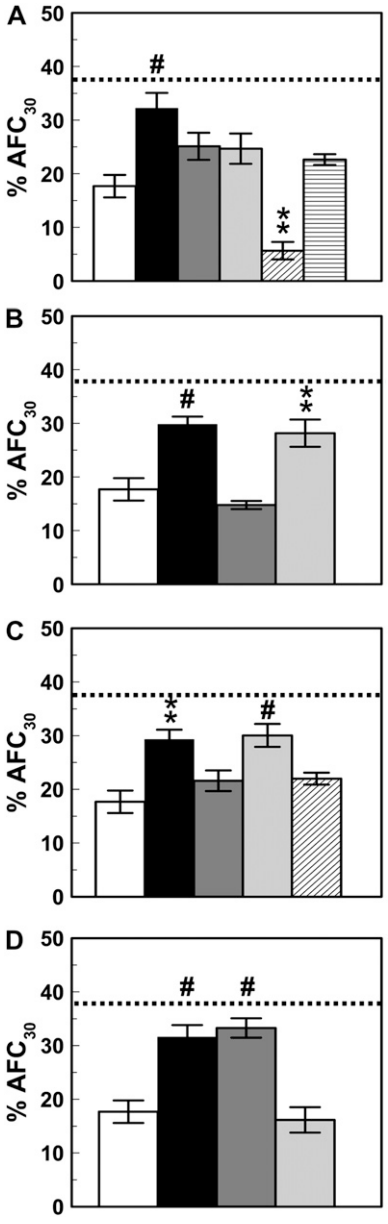


***Figure 4.*** Effect of blockade of the nucleotide–purinergic receptor axis on influenza A virus (IAV)–mediated inhibition of alveolar fluid clearance (AFC) at Day 2 after infection. (*A*) Effect of addition to the AFC instillate of the *de novo* pyrimidine synthesis inhibitor, A77–1726 (20 μM; n = 10) (*solid bar*), uridine (20 μM; n = 10) (*dark shaded bar*), A77–1726 with uridine (n = 9) (*light shaded bar*), A77–1726 with 1.5 mM amiloride (n = 8) (*diagonally hatched bar*), and genistein (20 μM; n = 6) (*horizontally hatched bar*) on AFC at Day 2 (no treatment, n = 11). (*B*) Effect of blockade of volume-regulated anion channels with fluoxetine (10 μM; n = 10) (*solid bar*), fluoxetine with 500 nM UTP (n = 7) (*dark shaded bar*), and Rho kinase inhibitor (50 μM; n = 9) (*light shaded bar*) on AFC at Day 2 (no treatment, n = 11). (*C*) Effect of purinolytic and pyrimidinolytic enzymes, apyrase (5 U/ml; n = 12) (*solid bar*), hexokinase (5 U/ml; n = 8) (*dark shaded bar*), UDP-glucose pyrophosphorylase with inorganic pyrophosphatase (both 5 U/ml; n = 11) (*light shaded bar*), and UDP-glucose pyrophosphorylase without inorganic pyrophosphatase (n = 9) (*hatched bar*) on AFC at Day 2 (no treatment, n = 11). AFC studies using hexokinase were performed in the presence of 10 mM glucose. AFC studies using UDP-glucose pyrophosphorylase were performed in the presence of 10 mM glucose-1-phosphate. (*D*) Effect of P2Y receptor antagonists suramin (200 μM; n = 7) (*solid bar*), XAMR-0721 (200 μM; n = 8) (*dark shaded bar*), and XAMR-0721 with 1.5 mM amiloride (n = 9) (*light shaded bar*) on AFC at Day 2 (no treatment, n = 11). *Dotted line* indicates mean AFC rate in untreated, mock-infected animals (n = 8). $^{**}P < 0.005$, $^{\#}P < 0.005$, compared with untreated, WSN-infected mice at Day 2.

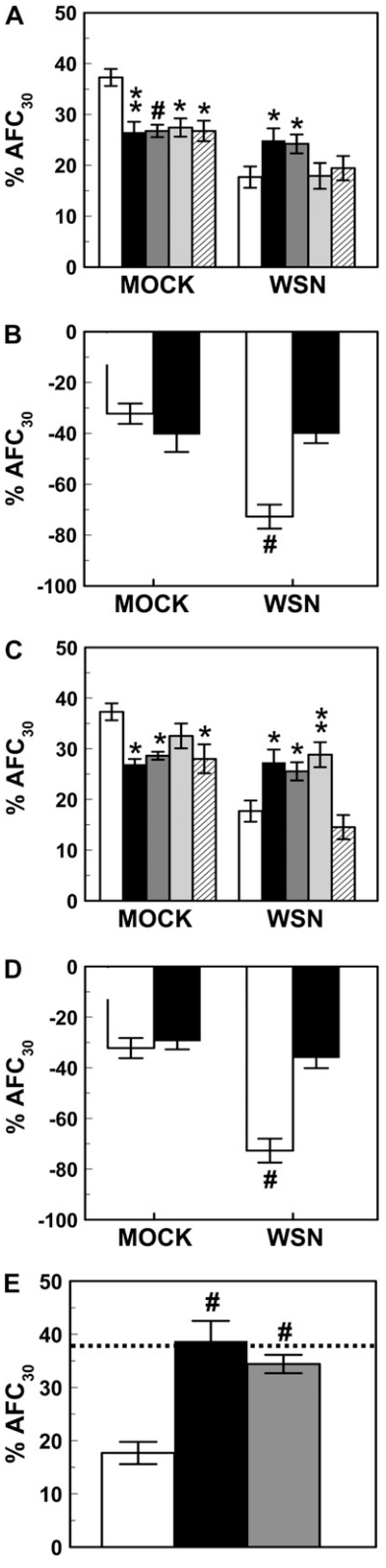


***Figure 5.*** Effect of influenza A virus infection for 2 days on anion secretion in BALB/c mice. (*A*) Effect of mock infection or infection with WSN virus on alveolar fluid clearance (AFC) sensitivity to the cystic fibrosis transmembrane regulator (CFTR) inhibitors, $CFTR_{inh}$-172 (*solid bars*) and glibenclamide (dark *shaded bars*), and the $Ca^{2+}$-activated $Cl^-$ channel inhibitors, niflumic acid (*light shaded bars*) and 4,4′-diisothiocyanostilbene-2,2′-disulfonic acid (DIDS) (*hatched bars*) (all 100 μM), at Day 2 (n = 8–12 per group). $^{*}P < 0.05$, $^{**}P < 0.005$, $^{\#}P < 0.0005$, compared with untreated mice (*open bars*) of the same infection status. (*B*) Effect of mock infection or infection with WSN virus on AFC in $Cl^-$-free ($Na^+$ gluconate) bovine serum albumin (BSA) in the absence (*open bars*) or presence (*solid bars*) of $CFTR_{inh}$-172 (100 μM) at Day 2 (n = 7–9 per group, except n = 11 for untreated, WSN-infected mice). $^{\#}P < 0.0005$ compared with untreated, mock-infected mice. (*C*) Effect of mock infection or infection with WSN virus on AFC sensitivity to the 5′ ectonucleotidase inhibitor, α,β-methyleneADP (100 μM) (*solid bars*), the $A_1$-AR antagonist, 8-SPT (200 μM) (*dark shaded bars*), the $A_1$-AR antagonist, DCPCX (100 μM) (*light shaded bars*), and the $A_{2b}$-adenosine receptor antagonist, MRS 1754 (100 μM) (*hatched bars*), at Day 2 (n = 8–9 per group, except n = 11 for untreated, WSN-infected mice). $^{*}P < 0.05$, $^{**}P < 0.005$, compared with untreated mice (*open bars*) of the same infection status. (*D*) Effect of mock infection or infection with WSN virus on AFC in $Cl^-$-free ($Na^+$ gluconate) BSA in the absence (*open bars*) or presence (*solid bars*) of 8-SPT (200 μM) at Day 2 (n = 9–11 per group). $^{\#}P < 0.0005$, compared with untreated, mock-infected mice. (*E*) Effect of 20 μM A77–1726 with 200 μM 8-SPT (n = 8) (*solid bar*) and 20 μM A77–1726 with 100 μM $CFTR_{inh}$-172 (n = 8) (*shaded bar*) on AFC at Day 2 (no treatment, n = 11). *Dotted line* indicates mean AFC rate in untreated, mock-infected animals (n = 12). $^{\#}P < 0.0005$ compared with untreated, WSN virus–infected mice.

the otherwise fully reversible degradation of UTP. The P2Y receptor antagonists, suramin and XAMR-0721 (both 200 μM), also reversed the inhibitory effect of WSN virus on basal AFC at Day 2 (Figure 4D); 1.5 mM amiloride completely inhibited the effect of XAMR-0721 on AFC at Day 2.

Because UTP and ATP levels are both high in BAL fluid from WSN virus–infected mice, relative to mock-infected mice (*see* Figure 3), but hexokinase does not reverse WSN virus–induced AFC inhibition, our data suggest that inhibition of AFC by WSN virus at Day 2 is mediated by UDP acting on epithelial $P2Y_6$ receptors. Indeed, in uninfected BALB/c mice, UDP was slightly more efficacious than UTP, and significantly

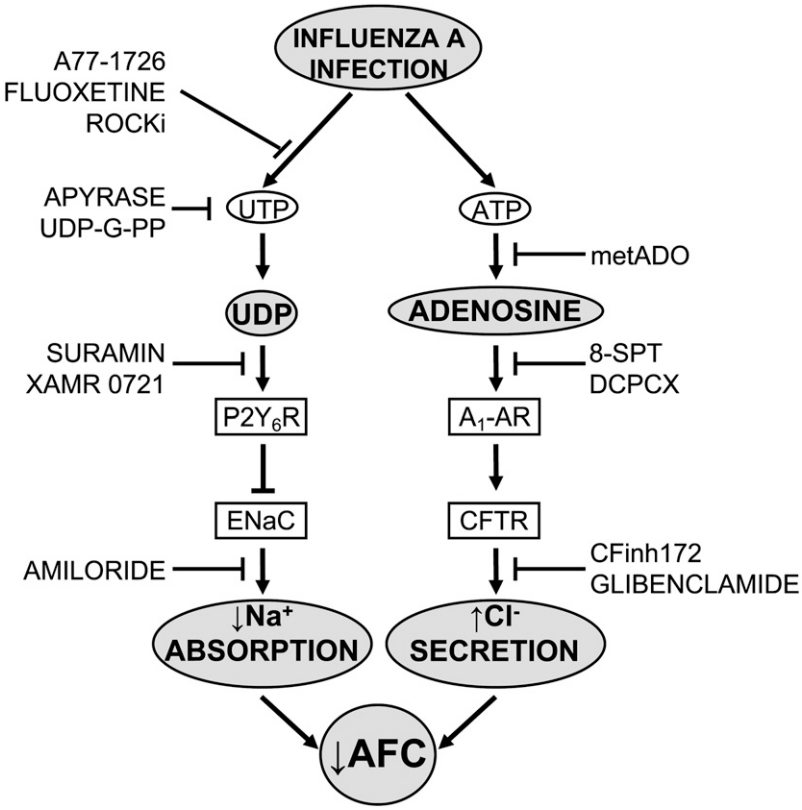


*Figure 6.* Proposed mechanism for inhibition of alveolar fluid clearance (AFC) after influenza A virus (IAV) infection of BALB/c mice. IAV infection results in increased release of the 5′-nucleotides, UTP and ATP, into the ALF. The UTP metabolite, UDP, activates $P2Y_6$-subtype purinergic receptors, resulting in inhibition of amiloride-sensitive epithelial $Na^+$ channels (ENaC) and reduced active $Na^+$ absorption. Concurrently, released ATP is metabolized by 5′ ectonucleotidases to adenosine, which activates $A_1$-subtype adenosine receptors ($A_1$-AR) and thereby stimulates bronchoalveolar epithelial $Cl^-$ secretion via the CFTR. Together, reduced $Na^+$ absorption and increased $Cl^-$ secretion result in severe impairment of AFC. Points of action of pharmacologic inhibitors used in the current study are also indicated: A77–1726 inhibits *de novo* pyrimidine synthesis; fluoxetine and ROCKi block opening of volume-regulated ion channels, which are the proposed release pathway for UTP; apyrase and UDP-glucose pyrophosphorylase (UDP-G-PP) prevent formation of UDP from UTP (by promoting formation of UMP and UDP-glucose from UTP, respectively); suramin and XAMR-0721 are P2Y purinergic receptor antagonists; amiloride inhibits ENaC activity; metADO inhibits 5′ ectonucleotidase–mediated hydrolysis of ATP to adenosine; 8-SPT and DCPCX are $A_1$-adenosine receptor antagonists; $CFTR_{inh}$-172 and glibenclamide are CFTR $Cl^-$ channel blockers.

more effective than ATP-γ-S (a nonhydrolyzable analog of ATP) in inhibiting AFC (Figure E4).

### Effect of IAV on Anion Secretion in BALB/c Mice

The CFTR $Cl^-$ channel inhibitors, $CFTR_{inh}$-172 and glibenclamide (both 100 μM), both inhibited AFC in mock-infected mice to a similar degree (Figure 5A). This indicates that AFC is normally in part dependent upon CFTR-mediated $Cl^-$ absorption in BALB/c mice (which is in agreement with prior studies [28]). At Day 2, both $CFTR_{inh}$-172 and glibenclamide increased the AFC rate to a level comparable to that in mock-infected, $CFTR_{inh}$-172–treated mice. $Ca^{2+}$-activated $Cl^-$ channel inhibitors (niflumic acid and DIDS, both 100 μM) had no significant effect on AFC at Day 2.

The AFC rate was significantly more negative in WSN virus–infected mice at Day 2 than in mock-infected mice under $Cl^-$-free conditions (in which NaCl in the instillate is replaced with $Na^+$ gluconate), which maximize the electrochemical gradient for $Cl^-$ secretion into the ALF (29) (Figure 5B). This increased fluid secretion could be reversed by $CFTR_{inh}$-172.

The 5′ ectonucleotidase inhibitor α, β-methyleneADP (100 μM), which blocks degradation of ATP to adenosine in the ALF (30), had an identical stimulatory effect on AFC to that of $CFTR_{inh}$-172 and glibenclamide at Day 2 (Figure 5C). The $A_1$-subtype adenosine receptor ($A_1$-AR) antagonists, 8-SPT (200 μM) and 1,3-dipropyl-8-cyclopentylxanthine (DCPCX) (100 μM), had a similar stimulatory effect on AFC at Day 2, but the $A_{2b}$-adenosine receptor antagonist, MRS 1754 (100 μM), did not. 8-SPT also blocked increased fluid secretion under $Cl^-$-free conditions in WSN virus–infected mice, confirming that increased $Cl^-$ efflux via CFTR at Day 2 results from $A_1$-AR activation (Figure 5D). Finally, concomitant blockade of IAV's inhibitory effect on amiloride-sensitive $Na^+$ absorption (using A77–1726) and its stimulatory effect on $Cl^-$ secretion (using either 8-SPT or $CFTR_{inh}$-172) had an additive effect, restoring normal AFC to infected mice (Figure 5E).

Taken together, these results indicate that impaired AFC at Day 2 after WSN virus infection results partially from adenosine activation of $A_1$-AR and the subsequent stimulation of CFTR-mediated $Cl^-$ secretion (*see* schematic in Figure 6).

### Effect of Adenylyl Cyclase Activation on WSN Virus–mediated Inhibition of AFC at Day 2 after Infection

β-Agonists can improve AFC in animal models of lung injury (31), and have shown promise prophylactically and therapeutically in humans with impaired AFC (32–34). However, IAV desensitizes β-adrenergic receptor (AR) in airway smooth muscle (35), and $A_1$-AR activation reduces intracellular cAMP levels (36). Both the adenylyl cyclase agonist, forskolin (50 μM), and the $\beta_2$-AR agonist, terbutaline (100 μM), increased mean AFC at Day 2 by stimulating amiloride-sensitive transport (Figure 7). These results indicate that, unlike after RSV infection (19), the bronchoalveolar epithelium remains sensitive to β-agonist stimulation in IAV-infected mice.

## DISCUSSION

The AFC process is crucial to efficient gas exchange in the lung (37), and patients with acute lung injury that have intact AFC have lower morbidity and mortality than those with compromised AFC (38). However, the effect of viral pathogens on respiratory epithelial $Na^+$ transport and AFC has not been studied in detail. Exposure of murine tracheal tissue to intact virus, or even viral antigens from pneumotropic IAV (6), results in rapid inhibition of active $Na^+$ transport (within 60 min). IAV also reduces ENaC activity in rat alveolar type II cells over a comparable time span (7). Nevertheless, it is not clear how

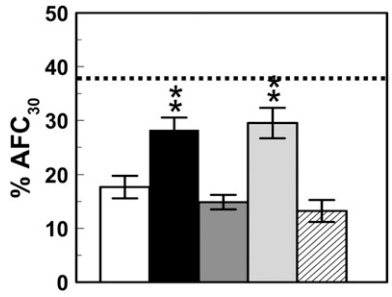


***Figure 7.*** Effect of adenylyl cyclase activation on influenza A virus–mediated inhibition of alveolar fluid clearance (AFC) at Day 2 after infection. Effect of 50 μM forskolin (n = 9) (*solid bar*), 50 μM forskolin with 1.5 mM amiloride (n = 8) (*dark shaded bar*), 100 μM terbutaline (n = 10) (*light shaded bar*), and 100 μM terbutaline with 1.5 mM amiloride (n = 7) (*hatched bar*) on AFC at Day 2 (no treatment, n = 11). *Dotted line* indicates mean AFC rate in untreated, mock-infected animals (n = 8). $^{**}P < 0.005$ compared with untreated, WSN-infected mice at Day 2.

such short-term effects correlate to the effects of viral replication within epithelial cells over a period of several days, as would happen in an infected subject.

Our current study is the first to demonstrate that any IAV strain has physiologically significant inhibitory effects on AFC *in vivo*. The short-term suppressive effect on AFC after infection with WSN virus for 1–4 hours is similar to the previously reported inhibitory effect of IAV on $Na^+$ transport in mouse tracheal tissue *in vitro* (6). Both effects can be induced by both live and UV-inactivated inocula (and so do not require viral replication), and both are mediated by activation of protein kinase C. In contrast, the long-term inhibitory effect of WSN virus on AFC requires active, high-level viral replication, and appears to be primarily mediated by release into the ALF of *de novo*–synthesized pyrimidine nucleotides and the subsequent activation of P2Y receptors, which reduces amiloride-sensitive AFC. This mechanism is similar to that described for RSV (11). However, unlike in RSV bronchiolitis, an additional component of net AFC impairment after long-term WSN virus infection results from WSN virus stimulation of $Cl^-$ secretion via $A_1$-AR–mediated activation of CFTR (Figure 6). This additional component may account for our finding that blockade of the purinergic nucleotide–P2Y receptor axis alone did not fully restore normal AFC in WSN virus–infected mice at Day 2, and may also explain why the AFC defect observed was more severe than that seen in RSV infection (11).

Epithelial necrosis and apoptosis is a component of IAV pneumonitis in mice (10), and the inhibitory effects of WSN virus on AFC might therefore simply be a consequence of viral cytopathic effect. However, our data indicate that the decline in AFC after WSN virus infection is unlikely to result solely, or even primarily, from destruction of the epithelial barrier by lytic viral replication, because a decline in AFC was detectable before evidence of significant epithelial cell death (either histologically or by analysis of BAL fluid and epithelial permeability). Moreover, a variety of data indicate that the respiratory epithelium retained its potential for normal AFC and was not necrotic, merely functionally impaired, at Day 2 after WSN virus infection: the absence of effect of WSN virus on amiloride-insensitive AFC (which indicates that inhibitory effects of WSN virus on both amiloride-sensitive and CFTR-mediated ion transport were selective); the stimulatory effect of WSN virus on CFTR-mediated fluid secretion under $Cl^-$-free conditions (which demonstrates that the bronchoalveolar epithelium remained capable of active ion transport); and, most importantly, the ability of a variety of pharmacologic agents with widely differing mechanisms of action (β-agonists, *de novo* pyrimidine synthesis inhibitors, VRAC inhibitors, P2Y receptor and AR antagonists, and enzymes that catabolize UTP) to reverse the inhibitory effect of WSN virus on amiloride-sensitive AFC at Day 2 within 30 minutes (the duration of the AFC procedure).

Our results suggest that IAV infection induces increased degradation of ALF ATP to adenosine, thereby activating $A_1$-AR and stimulating $Cl^-$ secretion via CFTR. They further suggest that, as in RSV infection (39), ectonucleotidase-mediated extracellular ATP hydrolysis may be enhanced after WSN virus infection. A stimulatory effect of IAV on anion secretion by respiratory epithelial cells has not previously been described. To our knowledge, there is also no previous report of adenosine receptor activation in response to infection with any pulmonary pathogen, although Factor and colleagues (40) have shown that adenosine can inhibit AFC in normal mice by activating $A_1$-AR on respiratory epithelial cells; our findings are in agreement with this study. $A_1$-AR antagonists can block endotoxin-induced lung injury (41) and prevent alveolar edema in ischemia–reperfusion–induced lung injury (42), which suggests that $A_1$-AR activation is proinflammatory and contributes to development of pulmonary edema in the inflamed lung. However, an antiinflammatory role for $A_1$-AR activation has also been described in adenosine-dependent pulmonary injury (43, 44). It is currently unclear whether the overall effect of adenosine in IAV infection is pro- or antiinflammatory.

Differences in expression of IAV receptors terminating in α2,3-linked and α2,6-linked sialic acid residues between airway epithelial cells from mice and humans (45) may result in disparities in cellular tropism for IAV at different levels of the respiratory tract (46), which may translate into divergent pathogenesis. Nevertheless, our data suggest that reduced capacity to clear bronchoalveolar fluid may be an unrecognized component of the pathogenesis of IAV pneumonitis, which contributes to development of pulmonary edema and hypoxemia. Moreover, our findings suggest that inhibition of *de novo* pyrimidine synthesis (and/or blockade of $A_1$-AR activation) might be of value therapeutically in alleviating hypoxemia in IAV pneumonitis, as it is in RSV infection (47, 48).

***Conflict of Interest Statement***: K.E.W. has no financial relationship with a commercial entity that has an interest in the subject of this manuscript. E.R.L. has no financial relationship with a commercial entity that has an interest in the subject of this manuscript. Z.P.T. has no financial relationship with a commercial entity that has an interest in the subject of this manuscript. E.N.Z.Y. has no financial relationship with a commercial entity that has an interest in the subject of this manuscript. N.A.J. has no financial relationship with a commercial entity that has an interest in the subject of this manuscript. R.K.D.'s minor child, Julian Durbin, owns stock in both Wyeth ($19,000) and Merck ($19,000). J.E.D.'s minor child, Julian Durbin, owns stock in both Wyeth ($19,000) and Merck ($19,000). I.C.D. has been granted U.S. Provisional Patent Application no. 60/573558: "Methods for using pyrimidine synthesis inhibitors to increase airway epithelial cell fluid uptake." (Filed May 21, 2004; Inventors: Drs. Ian C. Davis and Sadis Matalon) which converted to International PCT application (PCT/US2005/017939); May 2005; I.C.D. has received $500 in consultancy fees from Inspire Pharmaceuticals for advising on licensing issues related to this patent, and is the principal investigator for a grant from Inspire Pharmaceuticals, entitled: "Study of Inspire's therapeutic agents in murine model of respiratory syncytial virus infection and asthma" (11/01/2007–10/31/2008; $130,000, indirect plus direct costs); none of the experiments and results presented in this paper were funded from this grant.

***Acknowledgment***: The authors thank Dr. Estelle Cormet-Boyaka for her assistance with preparation of this manuscript.

## References

1. Lynch JP III, Walsh EE. Influenza: evolving strategies in treatment and prevention. *Semin Respir Crit Care Med* 2007;28:144–158.
2. Taubenberger JK, Morens DM, Fauci AS. The next influenza pandemic: can it be predicted? *JAMA* 2007;297:2025–2027.
3. Simonsen L, Taylor RJ, Viboud C, Miller MA, Jackson LA. Mortality benefits of influenza vaccination in elderly people: an ongoing controversy. *Lancet Infect Dis* 2007;7:658–666.

4. Davis IC, Matalon S. Epithelial sodium channels in the adult lung: important modulators of pulmonary health and disease. *Adv Exp Med Biol* 2007;618:127–140.
5. Ware LB, Golden JA, Finkbeiner WE, Matthay MA. Alveolar epithelial fluid transport capacity in reperfusion lung injury after lung transplantation. *Am J Respir Crit Care Med* 1999;159:980–988.
6. Kunzelmann K, Beesley AH, King NJ, Karupiah G, Young JA, Cook DI. From the cover: influenza virus inhibits amiloride-sensitive $Na^+$ channels in respiratory epithelia. *Proc Natl Acad Sci USA* 2000;97: 10282–10287.
7. Chen XJ, Seth S, Yue G, Kamat P, Compans RW, Guidot D, Brown LA, Eaton DC, Jain L. Influenza virus inhibits ENaC and lung fluid clearance. *Am J Physiol Lung Cell Mol Physiol* 2004;287:L366–L373.
8. Davis IC, Wolk KE, Yu ENZ. Influenza A virus inhibits alveolar fluid clearance in BALB/c mice. *Am J Respir Crit Care Med* 2008;177:A802.
9. Garcia-Sastre A, Durbin RK, Zheng H, Palese P, Gertner R, Levy DE, Durbin JE. The role of interferon in influenza virus tissue tropism. *J Virol* 1998;72:8550–8558.
10. Jewell NA, Vaghefi N, Mertz SE, Akter P, Peebles RS Jr, Bakaletz LO, Durbin RK, Flano E, Durbin JE. Differential type I interferon induction by respiratory syncytial virus and influenza A virus *in vivo*. *J Virol* 2007;81:9790–9800.
11. Davis IC, Sullender WM, Hickman-Davis JM, Lindsey JR, Matalon S. Nucleotide-mediated inhibition of alveolar fluid clearance in BALB/c mice after respiratory syncytial virus infection. *Am J Physiol Lung Cell Mol Physiol* 2004;286:L112–L120.
12. Saldias FJ, Lecuona E, Comellas AP, Ridge KM, Sznajder JI. Dopamine restores lung ability to clear edema in rats exposed to hyperoxia. *Am J Respir Crit Care Med* 1999;159:626–633.
13. Liu T, Ye Z. Attenuating mutations of the matrix gene of influenza A/WSN/33 virus. *J Virol* 2005;79:1918–1923.
14. Rocha MJ, Chen Y, Oliveira GR, Morris M. Physiological regulation of brain angiotensin receptor mRNA in AT1a deficient mice. *Exp Neurol* 2005;195:229–235.
15. Sidwell RW, Huffman JH, Gilbert J, Moscon B, Pedersen G, Burger R, Warren RP. Utilization of pulse oximetry for the study of the inhibitory effects of antiviral agents on influenza virus in mice. *Antimicrob Agents Chemother* 1992;36:473–476.
16. LeVine AM, Hartshorn K, Elliott J, Whitsett J, Korfhagen T. Absence of SP-A modulates innate and adaptive defense responses to pulmonary influenza infection. *Am J Physiol Lung Cell Mol Physiol* 2002; 282:L563–L572.
17. Hennet T, Ziltener HJ, Frei K, Peterhans E. A kinetic study of immune mediators in the lungs of mice infected with influenza A virus. *J Immunol* 1992;149:932–939.
18. Quan FS, Huang C, Compans RW, Kang SM. Virus-like particle vaccine induces protective immunity against homologous and heterologous strains of influenza virus. *J Virol* 2007;81:3514–3524.
19. Davis IC, Xu A, Gao Z, Hickman-Davis JM, Factor P, Sullender WM, Matalon S. Respiratory syncytial virus induces insensitivity to β-adrenergic agonists in mouse lung epithelium *in vivo*. *Am J Physiol Lung Cell Mol Physiol* 2007;293:L281–L289.
20. Davis IC, Lazarowski ER, Hickman-Davis JM, Fortenberry JA, Chen FP, Zhao X, Sorscher E, Graves LM, Sullender WM, Matalon S. Leflunomide prevents alveolar fluid clearance inhibition by respiratory syncytial virus. *Am J Respir Crit Care Med* 2006;173:673–682.
21. Elder RT, Xu X, Williams JW, Gong H, Finnegan A, Chong AS. The immunosuppressive metabolite of leflunomide, A77 1726, affects murine T cells through two biochemical mechanisms. *J Immunol* 1997; 159:22–27.
22. Okada SF, O'Neal WK, Huang P, Nicholas RA, Ostrowski LE, Craigen WJ, Lazarowski ER, Boucher RC. Voltage-dependent anion channel-1 (VDAC-1) contributes to ATP release and cell volume regulation in murine cells. *J Gen Physiol* 2004;124:513–526.
23. Maertens C, Wei L, Voets T, Droogmans G, Nilius B. Block by fluoxetine of volume-regulated anion channels. *Br J Pharmacol* 1999;126:508–514.
24. Nilius B, Voets T, Prenen J, Barth H, Aktories K, Kaibuchi K, Droogmans G, Eggermont J. Role of Rho and Rho kinase in the activation of volume-regulated anion channels in bovine endothelial cells. *J Physiol* 1999;516:67–74.
25. Cressman VL, Lazarowski E, Homolya L, Boucher RC, Koller BH, Grubb BR. Effect of loss of P2Y(2) receptor gene expression on nucleotide regulation of murine epithelial Cl(−) transport. *J Biol Chem* 1999;274:26461–26468.
26. Brunschweiger A, Muller CE. P2 receptors activated by uracil nucleotides—an update. *Curr Med Chem* 2006;13:289–312.
27. Lazarowski ER, Paradiso AM, Watt WC, Harden TK, Boucher RC. UDP activates a mucosal-restricted receptor on human nasal epithelial cells that is distinct from the P2Y2 receptor. *Proc Natl Acad Sci USA* 1997;94:2599–2603.
28. Fang X, Fukuda N, Barbry P, Sartori C, Verkman AS, Matthay MA. Novel role for CFTR in fluid absorption from the distal airspaces of the lung. *J Gen Physiol* 2002;119:199–207.
29. Hebestreit A, Kersting U, Hebestreit H. Hypertonic saline inhibits luminal sodium channels in respiratory epithelium. *Eur J Appl Physiol* 2007;100:177–183.
30. Lazarowski ER, Boucher RC, Harden TK. Constitutive release of ATP and evidence for major contribution of ecto-nucleotide pyrophosphatase and nucleoside diphosphokinase to extracellular nucleotide concentrations. *J Biol Chem* 2000;275:31061–31068.
31. Mutlu GM, Factor P. Alveolar epithelial β2-adrenergic receptors. *Am J Respir Cell Mol Biol* 2008;38:127–134.
32. Sartori C, Allemann Y, Duplain H, Lepori M, Egli M, Lipp E, Hutter D, Turini P, Hugli O, Cook S, *et al.* Salmeterol for the prevention of high-altitude pulmonary edema. *N Engl J Med* 2002;346:1631–1636.
33. Perkins GD, McAuley DF, Thickett DR, Gao F. The β-agonist lung injury trial (BALTI): a randomized placebo-controlled clinical trial. *Am J Respir Crit Care Med* 2006;173:281–287.
34. Licker M, Tschopp JM, Robert J, Frey JG, Diaper J, Ellenberger C. Aerosolized salbutamol accelerates the resolution of pulmonary edema after lung resection. *Chest* 2008;133:845–852.
35. Henry PJ, Rigby PJ, Mackenzie JS, Goldie RG. Effect of respiratory tract viral infection on murine airway β-adrenoceptor function, distribution and density. *Br J Pharmacol* 1991;104:914–921.
36. Spicuzza L, Di MG, Polosa R. Adenosine in the airways: implications and applications. *Eur J Pharmacol* 2006;533:77–88.
37. Matthay MA, Folkesson HG, Clerici C. Lung epithelial fluid transport and the resolution of pulmonary edema. *Physiol Rev* 2002;82:569–600.
38. Ware LB, Matthay MA. Alveolar fluid clearance is impaired in the majority of patients with acute lung injury and the acute respiratory distress syndrome. *Am J Respir Crit Care Med* 2001;163:1376–1383.
39. Tarran R, Button B, Picher M, Paradiso AM, Ribeiro CM, Lazarowski ER, Zhang L, Collins PL, Pickles RJ, Fredberg JJ, *et al.* Normal and cystic fibrosis airway surface liquid homeostasis: the effects of phasic shear stress and viral infections. *J Biol Chem* 2005;280:35751–35759.
40. Factor P, Mutlu GM, Chen L, Mohameed J, Akhmedov AT, Meng FJ, Jilling T, Lewis ER, Johnson MD, Xu A, *et al.* Adenosine regulation of alveolar fluid clearance. *Proc Natl Acad Sci USA* 2007;104:4083–4088.
41. Neely CF, Jin J, Keith IM. A1-adenosine receptor antagonists block endotoxin-induced lung injury. *Am J Physiol* 1997;272:L353–L361.
42. Neely CF, Keith IM. A1 adenosine receptor antagonists block ischemia–reperfusion injury of the lung. *Am J Physiol* 1995;268:L1036–L1046.
43. Sun CX, Young HW, Molina JG, Volmer JB, Schnermann J, Blackburn MR. A protective role for the A1 adenosine receptor in adenosine-dependent pulmonary injury. *J Clin Invest* 2005;115:35–43.
44. Blackburn MR, Lee CG, Young HW, Zhu Z, Chunn JL, Kang MJ, Banerjee SK, Elias JA. Adenosine mediates IL-13-induced inflammation and remodeling in the lung and interacts in an IL-13–adenosine amplification pathway. *J Clin Invest* 2003;112:332–344.
45. Ibricevic A, Pekosz A, Walter MJ, Newby C, Battaile JT, Brown EG, Holtzman MJ, Brody SL. Influenza virus receptor specificity and cell tropism in mouse and human airway epithelial cells. *J Virol* 2006;80: 7469–7480.
46. van Riel D, Munster VJ, de Wit E, Rimmelzwaan GF, Fouchier RAM, Osterhaus ADME, Kuiken T. Human and avian influenza viruses target different cells in the lower respiratory tract of humans and other mammals. *Am J Pathol* 2007;171:1215–1223.
47. Davis IC, Lazarowski ER, Chen FP, Hickman-Davis JM, Sullender WM, Matalon S. Post-infection A77–1726 blocks pathophysiologic sequelae of respiratory syncytial virus infection. *Am J Respir Cell Mol Biol* 2007;37:379–386.
48. Peebles RS Jr, Moore ML. A mechanistic advance in understanding RSV pathogenesis, but still a long way from therapy. *Am J Respir Cell Mol Biol* 2007;37:375–377.